The Doniach diagram and hydrogenation of the ternary compounds CePdIn and CePdSn

2006 J. Phys.: Condens. Matter 18 1743

(http://iopscience.iop.org/0953-8984/18/5/026)

INSTITUTE OF PHYSICS PUBLISHING JOURNAL OF PHYSICS: CONDENSED MATTER

J. Phys.: Condens. Matter **18** (2006) 1743–1755 doi:10.1088/0953-8984/18/5/026

The Doniach diagram and hydrogenation of the ternary compounds CePdIn and CePdSn

B Chevalier[1], **A Wattiaux and J-L Bobet**

Institut de Chimie de la Matière Condensée de Bordeaux (ICMCB), CNRS [UPR 9048], Université Bordeaux 1, Avenue du Docteur A Schweitzer, 33608 Pessac Cedex, France

E-mail: chevalie@icmcb-bordeaux.cnrs.fr

Received 24 October 2005, in final form 5 December 2005
Published 20 January 2006
Online at stacks.iop.org/JPhysCM/18/1743

Abstract

The process of hydrogenation of the antiferromagnetic compounds CePdIn and CePdSn has been studied. Investigation of the new hydrides CePdInH and CePdSnH by means of x-ray powder diffraction reveals that they adopt the same crystal symmetry as the original intermetallic but the unit cell volume increases during the hydrogenation. Magnetization, electrical resistivity, thermoelectric power and ^{119}Sn Mössbauer spectroscopy measurements reveal that CePdInH and CePdSnH order antiferromagnetically below $T_N = 3.0(2)$ and 5.0(2) K respectively. Moreover, the physical properties of the hydrides are less influenced by the Kondo effect. The changes of the Néel temperature induced by H insertion are explained on the basis of Doniach's diagram considering the competition between Kondo and Ruderman–Kittel–Kasuya–Yosida interactions.

1. Introduction

Many intermetallics based on cerium are considered as strongly correlated electron systems (SCES) [1]. Their interesting physical properties such as valence fluctuations and heavy fermion behaviour, superconductivity, semiconductivity, non-Fermi liquid behaviour and quantum phase transitions result from the competition between the RKKY indirect interaction and the Kondo effect. These interactions depend on the constant of coupling J_{cf} between 4f(Ce) and conduction electrons and are defined by two temperatures: the indirect magnetic RKKY temperature T_{RKKY} proportional to J_{cf}^2 and the Kondo temperature T_K which exhibits an exponential dependence on J_{cf}. The competition between T_{RKKY} and T_K temperatures versus J_{cf} is qualitatively described by the well-known Doniach phase diagram presented in figure 1 [2]. J_{cf} depends both on the 4f(Ce)–conduction electron mixing (i.e. V_{cf}) and on the location of the 4f(Ce) levels (i.e. E_{4f}) relative to the Fermi level (i.e. E_F) and so J_{cf} is proportional to $V_{cf}^2/(E_F - E_{4f})$. Hence three ranges can be distinguished on the Doniach diagram:

[1] Author to whom any correspondence should be addressed.

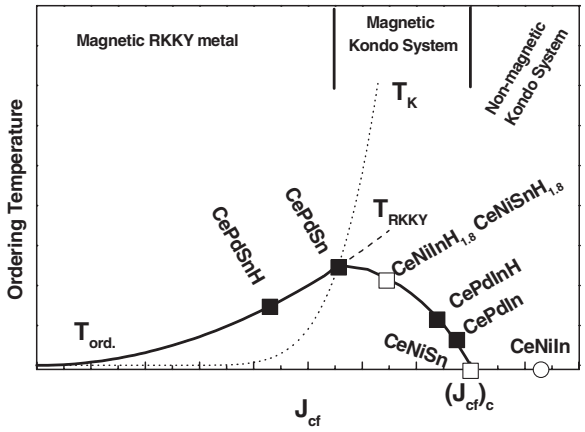

Figure 1. Doniach's diagram applied to the hydrogenation of CeTX compounds with T = Ni, Pd and X = In, Sn.

(i) if the 4f(Ce) levels lie deep below E_F, J_{cf} is small and the 4f(Ce) electrons stay in a normal localized state with a magnetic moment (magnetic RKKY metal);
(ii) when E_{4f} approaches E_F, J_{cf} increases and the compound begins to exhibit Kondo-like behaviour inducing a reduction of the ordered temperature and the magnetic moment (magnetic Kondo system);
(iii) with further increasing J_{cf}, ($J_{cf} > (J_{cf})_c$), the system goes into the non-magnetic valence fluctuation regime (non-magnetic Kondo system).

Using the low temperature properties, Fujita *et al* have located CeTIn and CeTSn (T = Ni or Pd) compounds on the Doniach diagram [3]. The two ternary compounds based on nickel do not exhibit magnetic ordering:

(i) CeNiIn is a valence fluctuating system having a high Kondo temperature (i.e. $T_K = 94$ K) estimated from specific heat measurements [4];
(ii) CeNiSn is an anisotropic dense Kondo compound forming a pseudogap in the density of states at the Fermi level [5].

Moreover, CeNiSn is close to the critical value $(J_{cf})_c$ as the application of uniaxial pressure [6] or slight substitution of Pd for Ni [7] induces the occurrence of an antiferromagnetic ordering. In contrast, the palladium based ternary compounds show antiferromagnetic ordering:

(i) CePdIn is a Kondo antiferromagnet with its Kondo temperature $T_K = 3.3$ K higher than its Néel temperature $T_N = 1.7$ K [4, 8];
(ii) CePdSn presents both a high ordered temperature $T_N = 7.5$ K and a smaller influence of the Kondo effect [9, 10].

(*This last point justifies CePdSn being presented in figure 1 close to the limit between the magnetic RKKY metal and the magnetic Kondo system.*) The replacement of Ni by bigger Pd in both CeNiIn and CeNiSn compounds induces the occurrence of a magnetic ordering. This agrees with the increase of the unit cell volume leading to a decrease of J_{cf}. Therefore, this last decrease is expected owing to the 'chemical expansion' effect.

Recently, we have shown that the hydrogenation of the intermetallics CeNiX (X = Al, Ga, In, Ge and Sn) also induces a decrease of J_{cf} [11]. For instance, the insertion of hydrogen into a sample of CeNiIn and CeNiSn reveals:

(i) an increase of the unit cell volume (respectively 9.6% and 7.85%);

(ii) a ferromagnetic transition below $T_C = 6.8(2)$ K ($CeNiInH_{1.8(1)}$) and $T_C = 7.0(2)$ K ($CeNiSnH_{1.8(2)}$) [12, 13].

In other words, the hydrogenation which induces the transition from an intermediate valence state (CeNiIn) or Kondo insulator behaviour (CeNiSn) to a ferromagnetic ordering can be considered as an application of 'negative' pressure on intermetallics.

In view of this, it is interesting to investigate the influence of the hydrogenation on the antiferromagnetic ordering of CePdIn and CePdSn. Considering the role of the Kondo effect in the physical properties of these two compounds, it could be assumed that the H insertion into CePdIn and CePdSn will induce respectively an increase and a decrease of the Néel temperature. In this paper, the crystallographic, electrical, thermoelectric and magnetic properties of the new hydrides $CePdInH_{1.0(1)}$ and $CePdSnH_{1.0(1)}$ are reported. Also, the investigation of $CePdSnH_{1.0(1)}$ by ^{119}Sn Mössbauer spectroscopy is presented and compared to that of CePdSn [14].

2. Experimental procedures

The samples CePdIn and CePdSn were synthesized by arc melting a stoichiometric mixture of pure elements (purity above 99.9%) in a high purity argon atmosphere. Then, the samples were turned and remelted several times to ensure homogeneity. An annealing treatment was carried out: one month at 1073 K, by enclosing the sample in evacuated quartz tubes.

Hydrogen absorption experiments were performed using the apparatus described previously [15]. An ingot of an annealed sample was heated under vacuum at 523 K for 12 h and then exposed for 48 h to 4 MPa of hydrogen gas. The amount of absorbed hydrogen was determined volumetrically by monitoring pressure changes in a calibrated volume.

X-ray powder diffraction with the use of a Philips 1050 diffractometer (Cu Kα radiation) was applied, before and after hydrogenation, for the characterization of the structural type and for the phase identification of the samples. The unit cell parameters were determined by a least squares refinement method using silicon (5N) as an internal standard. The crystal structures of the samples before and after hydrogenation were determined by Rietveld profile refinement using Fullprof software [16].

Magnetization measurements were performed using a superconducting quantum interference device (SQUID) magnetometer in the temperature range 1.8–370 K and applied fields up to 5 T. The electrical resistivity was determined above 4.2 K for a polycrystalline sample using standard dc four-probe measurements. For this investigation, the hydrides were compacted at room temperature (compactness $\cong$ 80%) in order to form a pellet (diameter = 6 mm and thickness = 3 mm) and then heated for 48 h at 523 K under 4 MPa pressure of hydrogen. Thermoelectric power measurements were performed on the same pellet using a dynamic method. Details of the cell used and measurement methods have been given previously [17].

^{119}Sn Mössbauer measurements were performed on CePdSn and its hydride between 4.2 and 300 K using a $CaSnO_3$ source and a conventional constant acceleration spectrometer. The isomer shifts (IS) were quoted relative to that of $CaSnO_3$ measured at room temperature. The samples contain 15 mg natural tin per cm^2. The spectra were fitted to the sums of Lorentzians by least squares refinements. All calculations were carried out without any constraint on the amplitudes and the widths.

Table 1. Crystallographic and magnetic data relating to the ternary compounds CePdIn and CePdSn and their hydrides.

	Crystallographic data					Magnetic data			
Compound	Type	a (Å)	b (Å)	c (Å)	V (Å)^3	μ_{eff} (μ_B mol^{-1})	θ_p (K)	T_N (K)	Reference
CePdIn	ZrNiAl	7.698		4.076	209.18	2.64	−41	1.65	[8]
CePdIn	ZrNiAl	7.686(2)		4.067(1)	208.07	2.59(2)	−42(1)		This work
CePdInH	**ZrNiAl**	**7.694(2)**		**4.199(1)**	**215.27**	**2.53(2)**	**−28(1)**	**3.0(2)**	This work
CePdSn	TiNiSi	7.526	4.7424	7.931	283.07	2.67	−68	7.5	[9]
CePdSn	TiNiSi	7.530(2)	4.698(1)	7.957(2)	281.49	2.56(2)	−72(1)	7.2(2)	This work
CePdSnH	**CeNiSnH**	**7.412(2)**	**4.531(1)**	**8.593(2)**	**288.59**	**2.74(2)**	**−29(1)**	**5.0(2)**	This work

3. Results and discussion

3.1. Preparation of hydrides and structural properties

Under the experimental conditions described previously (T = 523 K and $P(H_2)$ = 4 MPa), CePdIn and CePdSn absorb hydrogen; the hydrogenation induces a pulverization of the starting ingots. The amount of H atoms inserted is 1.0(1) per CePdIn or CePdSn formula. These hydrides are stable in ambient conditions.

The investigation of $CePdInH_{1.0}$ and $CePdSnH_{1.0}$ by means of x-ray powder diffraction reveals that the hydrides exhibit the same crystal symmetry as the original intermetallic. The unit cell parameters of these two series are compared in table 1. It is important to note that the hydrogenation significantly increases the unit cell volume V: respectively 3.5 and 2.5% after H insertion into the CePdIn and CePdSn lattices.

CePdInH crystallizes as the other hydrides $RENiInH_x$ (RE = La, Ce, Nd) in the hexagonal ZrNiAl-type structure where H atoms occupy the (RE_3Ni) tetrahedral sites [12, 18, 19]. However, the hydrogenation of CePdIn causes a pronounced anisotropic expansion of the unit cell: the a-parameter increases weakly (0.1%) whereas the c-parameter increases strongly (3.2%). For instance, the comparison of the x-ray powder pattern of CePdIn and its hydride (figure 2) evidences after hydrogenation a very small decrease of 2θ for Bragg reflections of a-dependent planes (300) and a strong decrease for c-dependent planes (002). Similar behaviour was observed during the hydrogenation of CeNiIn and was connected with the location of the H atoms in the (Ce_3Ni) tetrahedral sites along the c-axis. The full occupancy of these tetrahedral sites leads to the formation of the hydride $RENiInH_{1.33}$ [18, 19]. For CePdInH, the formula obtained indicates that only 75% of the sites (Ce_3Pd) are occupied. A similar result was observed for the deuterides $RENiInD_x$ (RE = La, Ce, Nd) demonstrating that the (RE_3Ni) sites can be partially filled [18].

CePdSnH is isomorphous to the hydride CeNiSnH showing a significant deformation of the orthorhombic TiNiSi-type structure [12, 20, 21]. In these hydrides, the cerium three-dimensional network can be described by an intergrowth of distorted trigonal (Ce_6) prisms surrounding alternately the Ni (or Pd) and Sn atoms. Moreover, in this structure, two types of chemically similar but geometrically different (Ce_3Ni or Ce_3Pd) tetrahedra are formed; only one that has a nearly regular Ce_3 side is fully occupied by a hydrogen atom [20]. The other significantly deformed (Ce_3Ni or Ce_3Pd) tetrahedron is empty. This hydrogen occupation agrees with the anisotropic expansion of the unit cell (table 1: the a- and b-parameters decrease by respectively −1.6 and −3.6% whereas the c-parameter increases strongly by 8.0%) as explained in the case of CeNiSnH [20].

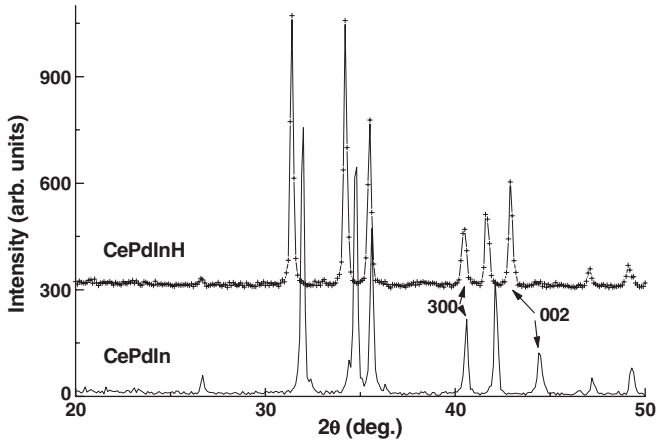

Figure 2. X-ray powder diffraction patterns of CePdIn and its hydride.

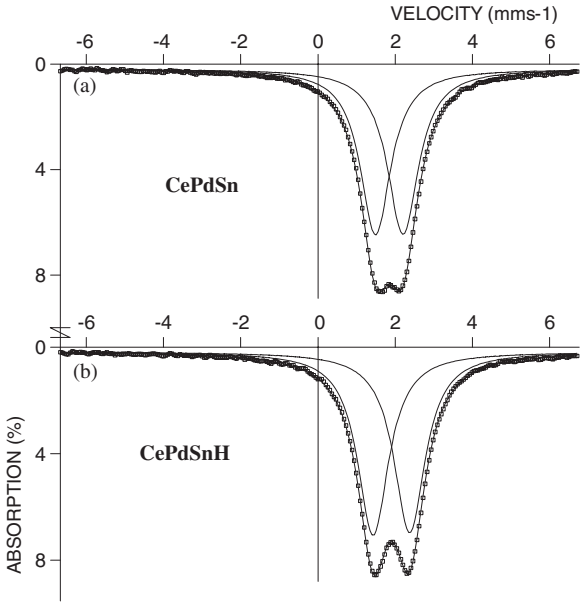

Figure 3. ^{119}Sn Mössbauer absorption spectra of CePdSn and CePdSnH measured at 293 K. The circles represent experimental values, while the lines are fits of the data.

In order to obtain more information on the evolution of the structural properties after hydrogenation, the $CePdSnH_y$ system ($y = 0$ and 1) has been investigated by ^{119}Sn Mössbauer spectroscopy. The spectra recorded at 293 K are shown in figure 3. The spectrum for CePdSn can be fitted as a symmetric quadrupole split doublet. QS $= 0.71(1)$ mm s^{-1} with a linewidth at half-height of $\Gamma = 0.97(1)$ mm s^{-1}. The isomer shift was determined as equal to IS $= 1.89(1)$ mm s^{-1}. The quadrupole splitting originates from the non-cubic local symmetry of Sn sites. The value of QS determined here is similar to that previously reported for this ternary stannide (QS $= 0.73$ mm s^{-1}) [14]. The value of IS is typical for a metal type Sn. For example for the parent stannide CeNiSn, crystallizing also in the orthorhombic TiNiSi

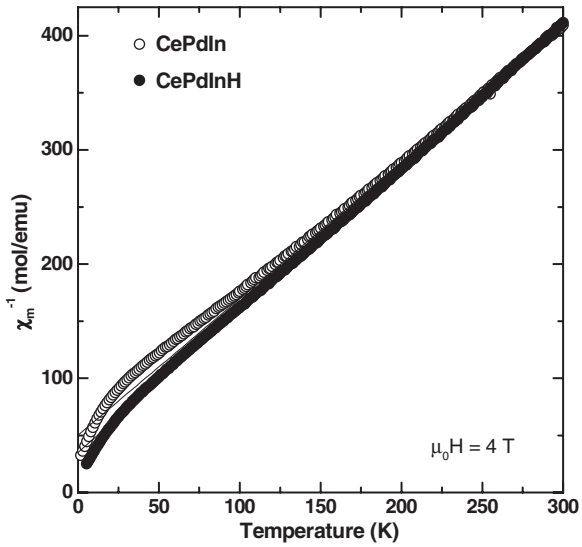

Figure 4. Temperature dependence of the reciprocal magnetic susceptibility, measured with an applied field $\mu_0 H = 4$ T, of CePdIn and its hydride.

type, IS = 1.900(6) mm s^{-1} at 293 K [22]. A symmetric quadrupole split doublet is also observed for the hydride CePdSnH, the Mössbauer parameters being IS = 1.94(1) mm s^{-1}, QS = 0.95(1) mm s^{-1} and Γ = 0.98(1) mm s^{-1}. At 293 K, IS increases in the sequence CePdSn → CePdSnH indicating an increase of the s electron density at the Sn nuclei. Similarly, QS increases in agreement with the presence of H atoms surrounding the Sn nuclei. In the other words, insertion of hydrogen in the CePdSn lattice strongly modifies the ^{119}Sn Mössbauer signals. Similar behaviour was reported by us during the study of the sequence CeNiSn → CeNiSnH [22].

3.2. Magnetic and electrical properties of CePdInH

Figure 4 compares the thermal dependence of the reciprocal magnetic susceptibility χ_m^{-1} of CePdIn and its hydride. Above 150 K, the data for CePdIn can be fitted with a Curie–Weiss law $\chi_m^{-1} = (T - \theta_p)/(0.125\ \mu_{eff}^2)$ giving $\theta_p = -42(1)$ K as the paramagnetic Curie temperature and $\mu_{eff} = 2.59(2)\ \mu_B$/Ce as the magnetic effective moment (table 1). These values are close to those reported previously (table 1) [8]. The $\chi_m^{-1} = f(T)$ curve for the hydride CePdInH also follows above 100 K a Curie–Weiss law with $\theta_p = -28(1)$ K and $\mu_{eff} = 2.53(2)\ \mu_B$/Ce. This last value agrees with that calculated for a free Ce^{3+} ion (2.54 μ_B). The increase of θ_p from $-42(1)$ to $-28(1)$ K in the sequence CePdIn → CePdInH suggests that the hydrogenation induces a decrease of the Kondo interaction.

Above 1.8 K, no anomaly attributed to the occurrence of a magnetic ordering transition can be detected via magnetization measurements performed on CePdIn (figure 5). This result confirms the low Néel temperature $T_N = 1.65$ K of this ternary indide determined by specific heat measurements [4, 8]. In contrast, the magnetic susceptibility of CePdInH exhibits a kink at $T_N = 3.0(2)$ K. This behaviour indicates that the hydride presents an antiferromagnetic ordering with a Néel temperature almost twice greater than that determined for the initial intermetallic. Similar increase of the magnetic ordering temperature after hydrogenation was evidenced for CePtAl; the Curie temperature increases from 5.6 to 11.6 K after H insertion [23].

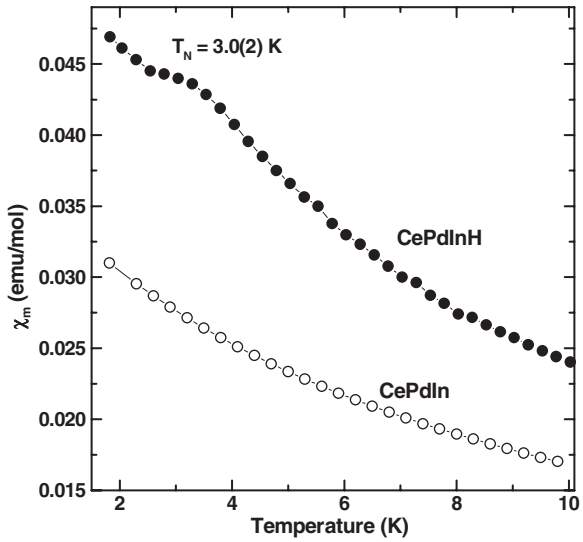

Figure 5. Temperature dependence of the magnetic susceptibility, measured with an applied field $\mu_0 H = 0.1$ T, of CePdIn and its hydride.

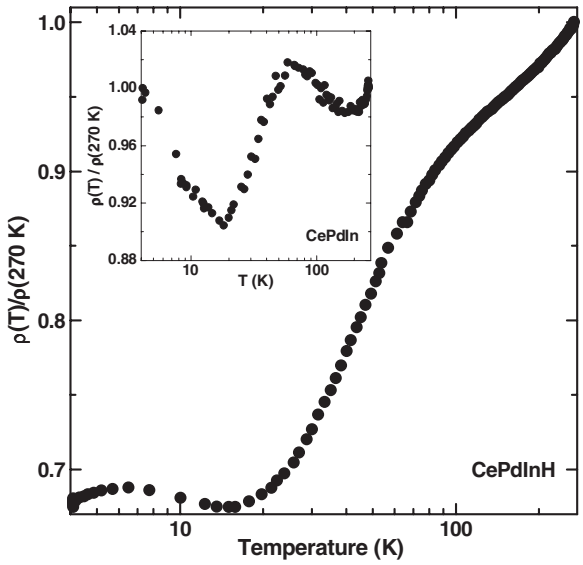

Figure 6. Reduced electrical resistivity as a function of log T for CePdIn (inset) and its hydride.

As shown in figure 6, the reduced electrical resistivity of CePdIn, measured between 4.2 and 270 K, is strongly modified by its hydrogenation. The curve $\rho(T)/\rho(270\ \mathrm{K}) = f(T)$ for CePdIn reveals several anomalies: (i) a broad maximum occurs around 64 K; (ii) below this maximum, $\rho(T)$ decreases and a minimum appears near 18 K; (iii) finally, below this minimum there is a rise of $\rho(T)$ down to 4.2 K (inset in figure 6). In the two temperature ranges 80–190 and 4.2–12 K, the law $\rho(T)/\rho(270\ \mathrm{K}) = -A \log T$ (A = constant) is observed. Such behaviours, which agree with those reported for a polycrystalline sample of CePdIn [8, 24],

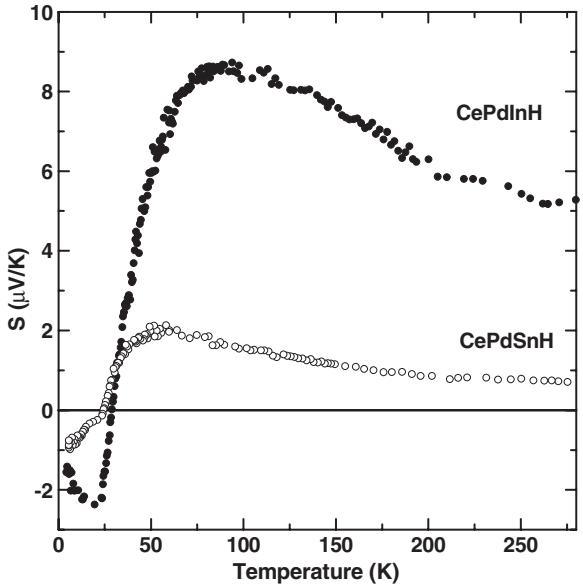

Figure 7. Temperature dependence of the thermoelectric power of the hydrides CePdInH and CePdSnH.

are expected for Kondo-type interactions in the presence of crystal field effects [25]. The high temperature logarithmic regime represents the Kondo effect in the excited doublet, whereas the low temperature region is related to the Kondo effect from the crystal field ground state (incoherent Kondo scattering). As the measurements were performed above 4.2 K (i.e. higher than the Néel temperature $T_N = 1.65$ K), no decrease is evidenced at lower temperature. The curve for the hydride CePdInH shows different characteristics: (i) a downward curvature around 60–80 K associated with a crystal field effect; (ii) a minimum at 14 K and a maximum near 6 K. The minima at 18 and 14 K for CePdIn and its hydride respectively are related to the Kondo effect from the crystal field ground state. Such a decrease (18 K $\rightarrow$ 14 K) indicates that the Kondo effect decreases with H insertion. Also, the decrease of $\rho(T)$ below 6 K for CePdInH could be associated with the loss of spin disorder scattering of the conduction electrons owing to the appearance of an antiferromagnetic transition (detected around 3.0(2) K as shown previously by magnetization measurements).

Figure 7 shows the temperature dependence of the thermoelectric power S of CePdInH. This curve $S = f(T)$ exhibits many similarities to that reported for the initial indide CePdIn [26]. It is mainly characterized by the existence of two extremes: a positive maximum of about 9 μV K^{-1} near 90 K and a negative one at -2.5 μV K^{-1} around 16 K. Between them, the thermoelectric power is equal to 0 at 28 K. Such behaviour is commonly observed for Ce based Kondo lattice systems having a low Kondo temperature such as $CeAl_2$ [27]. The broad positive peak is ascribed to an interplay of the Kondo and the crystalline electric field (CEF) effects [28]. The peak height measures the strength of the Kondo effect, and the peak temperature measures the CEF splitting. The temperature $\cong$90 K of the positive maximum for CePdInH, is comparable to that where the curve $\rho(T)/\rho(270\text{ K}) = f(T)$ (figure 6) exhibits a downward curvature maximum. Meanwhile, the origin of the negative peak (16 K) is ascribed by Sakurai *et al* [29] to an interplay of the Kondo effect and the onset of the short range magnetic correlation. Finally, it is interesting to note that the value of $S \cong 32$ μV K^{-1} for

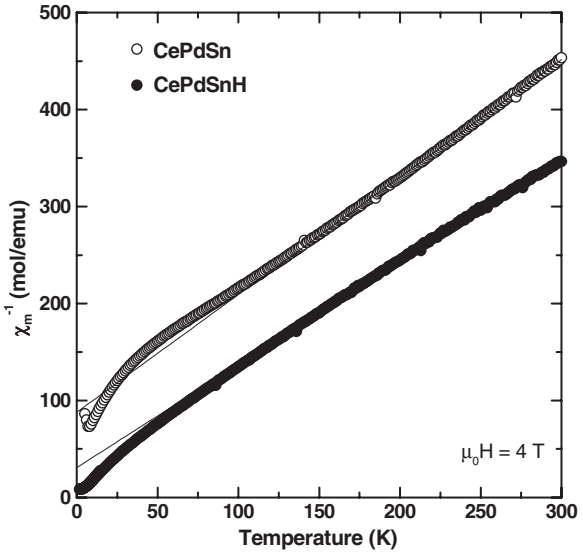

Figure 8. Temperature dependence of the reciprocal magnetic susceptibility, measured with an applied field $\mu_0 H = 4$ T, of CePdSn and its hydride.

the broad positive peak in CePdIn [26] is higher than that determined here (9 μV K^{-1}) for CePdInH, suggesting a diminution of the strength of the Kondo effect.

The magnetization and transport measurements performed on the hydride CePdInH reveal that the H insertion in CePdIn decreases the influence of the Kondo effect and consequently the Néel temperature increases.

3.3. Magnetic and electrical properties of CePdSnH

The curves $\chi_m^{-1} = f(T)$ relating to the reciprocal magnetic susceptibility of CePdSn and CePdSnH are shown in figure 8. Above 100 K, the data are on straight lines, obeying the Curie–Weiss law. The effective moments μ_{eff} for CePdSn and CePdSnH are 2.56(2) μ_B/Ce and 2.74(2) μ_B/Ce respectively (table 1) which are close to the value for free Ce^{3+}. The deviation from the Curie–Weiss law below 100 K is due to the crystal electric field effect. In this case also, θ_p shows a significant decrease in magnitude for the sequence CePdSn $\rightarrow$ CePdSnH (table 1). This may be due to a decrease of the hybridization effect between 4f(Ce) electrons and conduction ones.

The magnetic susceptibility χ_m at low temperatures, for CePdSnH and CePdSn, is plotted in figure 9. The peaks of $\chi_m = f(T)$ are identified as the Néel temperature T_N. The hydrogenation of CePdSn induces a decrease of T_N from 7.2(2) to 5.0(2) K. Certainly, the hydrogenation also changes the magnetic structure of CePdSn. At 2 K and up to $\mu_0 H \leqslant 4.8$ T, in the antiferromagnetic range, the magnetization of CePdSn increases linearly with the applied magnetic field (figure 10). In contrast, below $T_N = 5.0(2)$ K the magnetization of the hydride CePdSnH increases linearly at low fields, shows a steep rise in the range 0.6–1.4 T and then exhibits a tendency to saturation. This behaviour is typical of a magnetic transition induced by the applied magnetic field; at 2 and 4 K, the critical field is estimated respectively at 1.2(2) and 0.8(2) T.

Above 30 K, the reduced resistivity of CePdSn (figure 11) does not vary linearly with temperature (as for a normal metal) and the curve $\rho(T)/\rho(270\ \text{K}) = f(T)$ presents

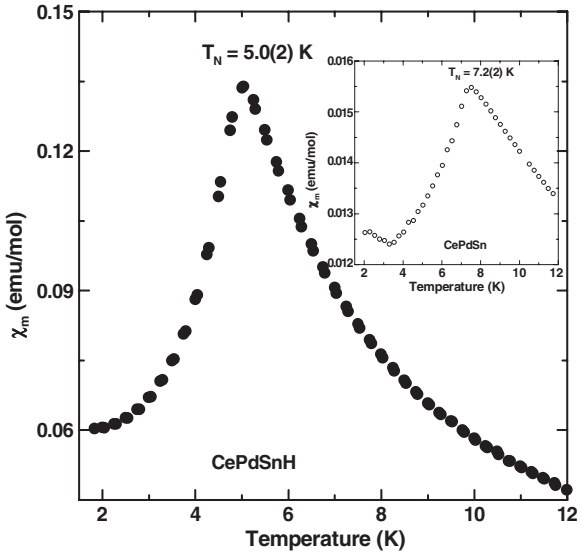

Figure 9. Temperature dependence of the magnetic susceptibility, measured with an applied field $\mu_0 H = 0.1$ T, of CePdSnH and CePdSn (inset).

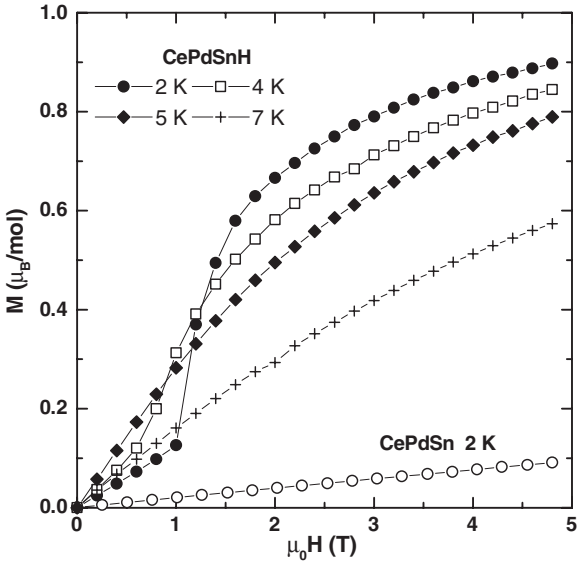

Figure 10. Field dependence of the magnetization of CePdSn at 2 K and its hydride at temperatures between 7 and 2 K.

a downward curvature associated with a crystal field effect which becomes temperature dependent in the paramagnetic range. At low temperatures its reduced resistivity increases slightly between 20 and 7.3(2) K and then decreases strongly. This behaviour is typical of a magnetically ordered Kondo system showing the presence of crystal field spitting of the 4f(Ce) electron. No similar anomaly can be detected from the curve $\rho(T)/\rho(270\ \mathrm{K}) = f(T)$ for CePdSnH; a linear variation is observed above 50 K, and a tendency to saturation

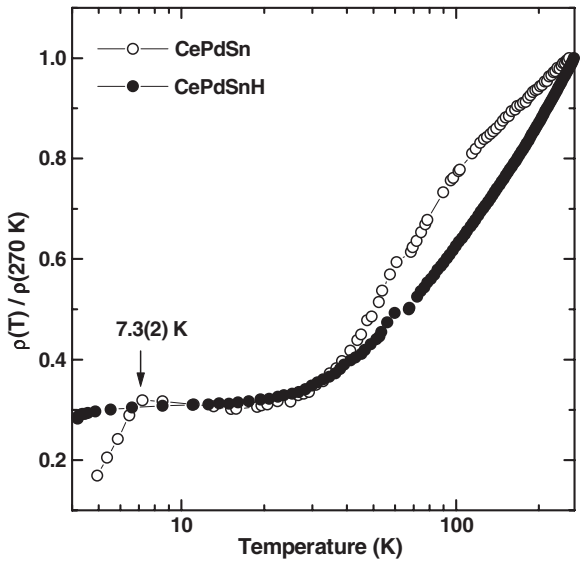

Figure 11. Reduced electrical resistivity as a function of log T for CePdSn and its hydride.

appears between 30 and 5 K where the beginning of a decrease occurs (the appearance of the antiferromagnetic ordering). This strikingly different behaviour of hydride indicates the absence of the Kondo scattering found in CePdSn.

The curve $S = f(T)$ for CePdSnH (figure 7) agrees with a small influence of the Kondo effect on its physical properties. This curve can be compared to that reported previously for the ternary stannide CePdSn [14] where a similar positive peak was observed; but the temperature of this maximum decreases from 110 to 60 K and the value of S at this peak diminishes from 8 to 2.5 μV K^{-1} in the sequence CePdSn $\rightarrow$ CePdSnH. These two decreases are correlated with the diminution of the Kondo effect during the hydrogenation of CePdSn.

Similar comparison of the curves $S = f(T)$ observed for the two hydrides CePdInH and CePdSnH (figure 7) reveals that the influence of the Kondo effect decreases from CePdInH to CePdSnH. Indeed, the temperature of the positive maximum decreases from 90 to 60 K and the S value at these temperatures from 9 to 2.5 μV K^{-1}.

At 4.2 K, in the antiferromagnetic state, the ^{119}Sn Mössbauer spectra corresponding to CePdSn and CePdSnH (figure 12) are very broad in comparison with those obtained at room temperature (figure 3) or in the paramagnetic range of these compounds. (*For instance, the spectra width at half-height for hydride CePdSnH increases weakly from 10.7 to 6.1 K* (*2.19* $\rightarrow$ *2.25 mm s*$^{-1}$) *and strongly at lower temperatures; 2.50 and* 2.65 *mm s*$^{-1}$ *respectively at 4.8 and 4.2 K*). These broadenings can be explained in terms of a transferred magnetic field that would appear if the antiferromagnetic arrangement of Ce moments led to the creation of a hyperfine field H_{hf} at the Sn nuclei (*the spectra width at half-height increases significantly below 7.5(5) and 5.5(5) K respectively for CePdSn and CePdSnH, in agreement with the occurrence of their antiferromagnetic ordering*). This agrees with the case for CePdSn which presents an incommensurate magnetic structure [10]. However, the sextuplet characteristic of magnetic hyperfine interaction is still unresolved due to the relatively low value of H_{hf}, respectively equal to 1.45 and 1.15 T for CePdSn and its hydride. The determination of the magnetic structure of CePdSnH by means of neutron powder diffraction is necessary in order to explain this hyperfine field splitting.

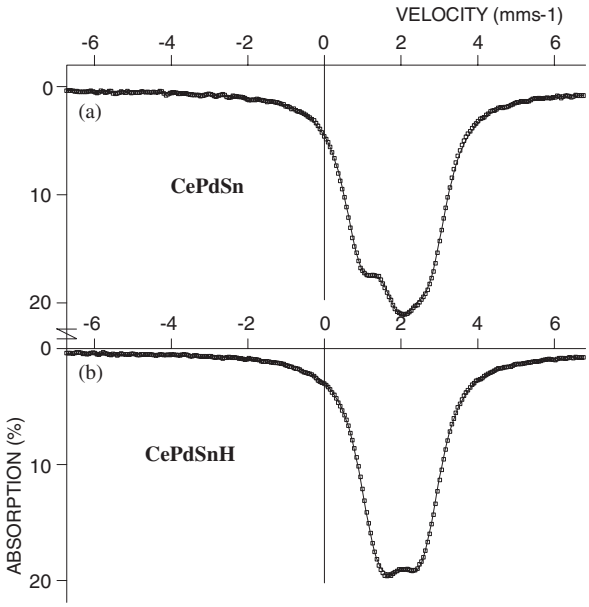

Figure 12. ^{119}Sn Mössbauer absorption spectra of CePdSn and CePdSnH measured at 4.2 K. The circles represent experimental values, while the lines are fits to the data.

4. Conclusion

H insertion into the ternary compounds CePdIn and CePdSn:

(i) allows one to obtain the new hydrides CePdInH and CePdSnH which crystallize with the same crystal symmetry as the parent compounds;
(ii) induces an increase of the unit cell volume, by 3.5% and 2.5% in the cases of CePdIn and CePdSn respectively;
(iii) modifies their magnetic antiferromagnetic properties: T_N increases in the sequence CePdIn $\rightarrow$ CePdInH but decrease for CePdSn $\rightarrow$ CePdSnH;
(iv) diminishes the influence of the Kondo effect on their physical properties.

In other words, in these cases the hydrogenation can be compared to the application of a 'negative' pressure inducing a decrease of the J_{cf} interaction.

The change of the physical properties resulting from the hydrogenation of CeTX compounds (T = Ni, Pd and X = In, Sn) can be explained on the basis of the Doniach diagram (figure 1). The hydrogen insertion into:

(i) a non-magnetic Kondo system (CeNiIn, CeNiSn) leads to a magnetically ordered hydride ($CeNiInH_{1.8}$, $CeNiSnH_{1.8}$);
(ii) a magnetic Kondo system strongly (CePdIn) or weakly (CePdSn) influenced by the Kondo effect induces an increase or a decrease of the Néel temperature.

Acknowledgment

The authors would like to thank R Decourt for his assistance during the electrical resistivity and thermoelectric power measurements.

References

[1] Edestein A S 2003 *J. Magn. Magn. Mater.* **256** 430
[2] Doniach S 1977 *Physica* B **91** 231
[3] Fujita T, Suzuki T, Nishigori S, Takabatake T, Fujii H and Sakurai J 1992 *J. Magn. Magn. Mater.* **108** 35
[4] Satoh K, Fujita T, Maeno Y, Uwatoko Y and Fujii H 1990 *J. Phys. Soc. Japan* **59** 692
[5] Takabatake T, Teshima F, Fujii H, Nishigori S, Suzuki T, Fujita T, Yamaguchi Y, Sakurai J and Jaccard D 1990 *Phys. Rev.* B **41** 9607
[6] Umeo K, Igaue T, Chyono H, Echizen Y, Kosaka T and Uwatoko Y 1999 *Phys. Rev.* B **60** R6957
[7] Kasaya M, Tani T, Suzuki H, Ohoyama K and Kohgi M 1991 *J. Phys. Soc. Japan* **60** 2542
[8] Brück E, Van Sprang M, Klaesse J C P and De Boer F R 1988 *J. Appl. Phys.* **63** 3417
[9] Adroja D T, Malik S K, Padalia B D and Vijayaraghavan R 1988 *Solid State Commun.* **66** 1201
[10] Kasaya M, Tani T, Ohoyama K, Kohgi M and Isikawa Y 1992 *J. Magn. Magn. Mater.* **104–107** 665
[11] Chevalier B, Pasturel M, Bobet J-L, Decourt R, Etourneau J, Isnard O, Sanchez Marcos J and Rodriguez Fernandez J 2004 *J. Alloys Compounds* **383** 4
[12] Chevalier B, Kahn M L, Bobet J-L, Pasturel M and Etourneau J 2002 *J. Phys.: Condens. Matter* **14** L365
[13] Chevalier B, Bobet J-L, Pasturel M, Bauer E, Weill F, Decourt R and Etourneau J 2003 *Chem. Mater.* **15** 2181
[14] Sakurai J, Yamaguchi Y, Mibu K and Shinjo T 1990 *J. Magn. Magn. Mater.* **84** 157
[15] Bobet J-L, Pechev S, Chevalier B and Darriet B 1998 *J. Alloys Compounds* **267** 136
[16] Rodriguez-Carvajal J 1993 *Physica* B **192** 55
[17] Dordor P, Marquestaut E and Villeneuve G 1980 *Rev. Phys. Appl.* **15** 1607
[18] Yartys V A, Denys R V, Hauback B C, Fjellvag H, Bulyk I I, Riabov A B and Kalychak Y A M 2002 *J. Alloys Compounds* **330–332** 132
[19] Denys R V, Riabov A B, Yartys V A, Hauback B C and Brinks H W 2003 *J. Alloys Compounds* **356/357** 65
[20] Yartys V A, Ouladdiaf B, Isnard O, Khyzhun O Yu and Buschow K H J 2003 *J. Alloys Compounds* **359** 62
[21] Chevalier B, Pasturel M, Bobet J-L, Etourneau J, Isnard O, Sanchez Marcos J and Rodriguez Fernandez J 2004 *J. Magn. Magn. Mater.* **1** 576
[22] Chevalier B, Wattiaux A, Fournès L and Pasturel M 2004 *Solid State Sci.* **6** 573
[23] Bobet J-L, Chevalier B, Weill F and Etourneau J 2002 *J. Alloys Compounds* **330–332** 373
[24] Brück E, Nakotte H, Bakker K, de Boer F R, de Chatel P F, Li J-Y, Kuang J P and Yang F-M 1993 *J. Alloys Compounds* **200** 79
[25] Cornut B and Coqblin B 1972 *Phys. Rev.* B **5** 4541
[26] Yamaguchi Y, Sakurai J, Teshima F, Kawanaka H, Takabatake T and Fujii H 1990 *J. Phys.: Condens. Matter* **2** 5715
[27] Garde C S and Ray J 1995 *Phys. Rev.* B **51** 2960
[28] Bhattacharjee A K and Coqblin B 1976 *Phys. Rev.* B **13** 3441
[29] Sakurai J, Takagi H, Kuwai T and Isikawa Y 1998 *J. Magn. Magn. Mater.* **177–181** 407